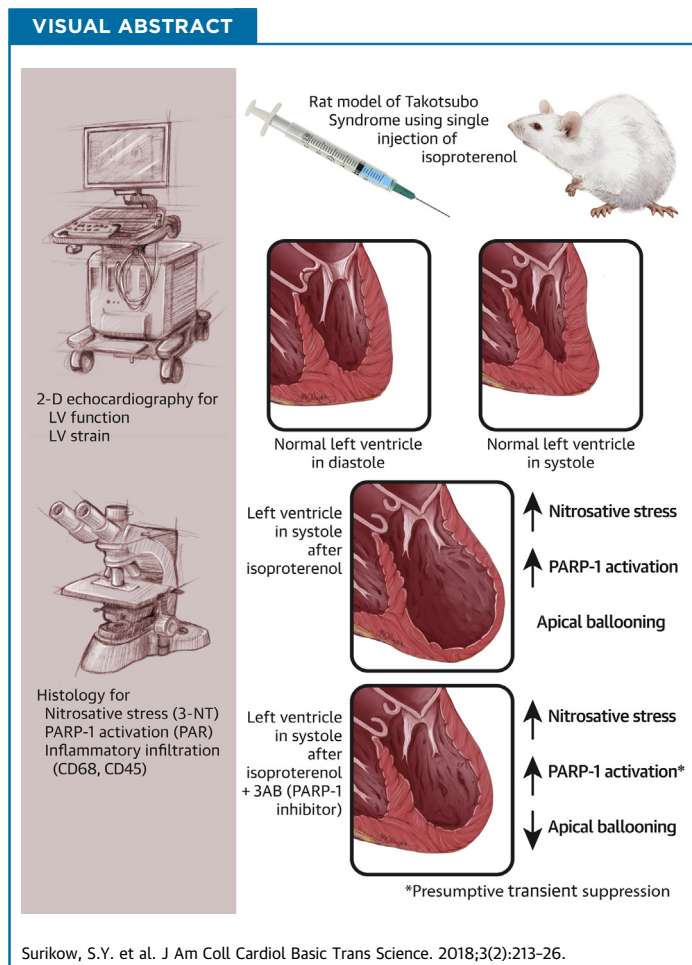


PRECLINICAL RESEARCH

# Nitrosative Stress as a Modulator of Inflammatory Change in a Model of Takotsubo Syndrome



Sven Y. Surikow, BHLTHSc (HONS),<sup>a,b</sup> Thanh H. Nguyen, MD, MMEDSCI, PhD,<sup>a,b</sup> Irene Stafford, BSc,<sup>a</sup> Matthew Chapman, BSc, MCLINSCI, DMU, CEPIA,<sup>a</sup> Sujith Chacko, MBBS,<sup>a</sup> Kuljit Singh, MBBS, PhD,<sup>a,b</sup> Giovanni Licari, BSc, PhD,<sup>b</sup> Betty Raman, MBBS,<sup>a,b</sup> Darren J. Kelly, PhD,<sup>c</sup> Yuan Zhang, MBBS, PhD,<sup>c</sup> Mark T. Waddingham, BSc (HONS), PhD,<sup>c</sup> Doan T. Ngo, BPHARM, PhD,<sup>a</sup> Alexander P. Bate,<sup>a</sup> Su Jen Chua, MBBS,<sup>a</sup> Michael P. Frenneaux, MD,<sup>d</sup> John D. Horowitz, MBBS, BMEDSCI(HONS), PhD<sup>a,b</sup>



**HIGHLIGHTS**

- Treatment of female rats with a single dose of isoproterenol results in apical hypokinesis mimicking Takotsubo syndrome
- Myocardial inflammation includes increased content of 3-nitrotyrosine and poly(ADP-ribose), indicating nitrosative stress and PARP-1 activation, respectively
- Pretreatment with 3-aminobenzamide (a PARP-1 inhibitor) attenuates negative inotropic changes
- We conclude that the peroxynitrite/ PARP-1 cascade contributed to negative inotropy in this model of Takotsubo syndrome, consistent with the limited data available in patients

From <sup>a</sup>The Queen Elizabeth Hospital, Department of Cardiology, University of Adelaide, South Australia, Australia; <sup>b</sup>Basil Hetzel Institute, Adelaide, South Australia, Australia; <sup>c</sup>Department of Medicine, St. Vincent's Hospital, University of Melbourne, Melbourne, Australia; and the <sup>d</sup>University of East Anglia, Norfolk, United Kingdom. This work was funded in part by a Project Grant from the

ABBREVIATIONS  
AND ACRONYMS

**3AB** = 3-aminobenzamide  
**ANOVA** = analysis of variance  
**ISO** = isoproterenol  
**LV** = left ventricular  
**NF- $\kappa$ B** = nuclear factor kappa B  
**NO** = nitric oxide  
**NOS** = nitric oxide synthase  
**NT** = nitrotyrosine  
**O<sub>2</sub><sup>-</sup>** = superoxide  
**ONOO<sup>-</sup>** = peroxynitrite  
**PAR** = poly(ADP-ribose)  
**PARP** = poly(ADP-ribose) polymerase  
**TS** = Takotsubo syndrome  
**TXNIP** = thioredoxin-interacting protein

## SUMMARY

Previous studies have shown that patients with Takotsubo syndrome (TS) have supranormal nitric oxide signaling, and post-mortem studies of TS heart samples revealed nitrosative stress. Therefore, we first showed in a female rat model that isoproterenol induces TS-like echocardiographic changes, evidence of nitrosative stress, and consequent activation of the energy-depleting enzyme poly(ADP-ribose) polymerase-1. We subsequently showed that pre-treatment with an inhibitor of poly(ADP-ribose) polymerase-1 ameliorated contractile abnormalities. These findings thus add to previous reports of aberrant  $\beta$ -adrenoceptor signaling (coupled with nitric oxide synthase activation) to elucidate mechanisms of impaired cardiac function in TS and point to potential methods of treatment. (J Am Coll Cardiol Basic Trans Science 2018;3:213–26)  
 © 2018 The Authors. Published by Elsevier on behalf of the American College of Cardiology Foundation. This is an open access article under the CC BY-NC-ND license (<http://creativecommons.org/licenses/by-nc-nd/4.0/>).

**T**akotsubo syndrome (TS) reflects catecholamine-induced global myocardial inflammation, which predominantly affects the left ventricular (LV) apex. Since its initial description by

Japanese investigators (1), the phenomenon of TS has aroused considerable interest among clinicians, as its differentiation from acute myocardial infarction represents a diagnostic challenge (2,3). Even more intriguing is the epidemiology of TS, with its predominant occurrence in aging women, episodes being precipitated both by acute emotional or physical stressors and the presence of neuropsychiatric disorders (4,5). Furthermore, it was originally considered that TS might be a relatively rare disorder, which is not the case: approximately 10% of suspected

SEE PAGE 227

ST-segment elevation myocardial infarction cases in women aged >50 years are actually TS (6). Finally, TS induces prolonged myocardial inflammation (7), including patchy inflammatory infiltrate on myocardial biopsy samples (8), with persistent LV dysfunction (9), disordered cardiac energetics (10), and associated impairment of quality of life for  $\geq 3$  months, with a propensity toward recurrence (11).

To date, the only definitive progress that has been made regarding the pathogenesis of TS is related to the pivotal role of catecholamine release and its interactions with the myocardium: there is extensive evidence that TS can be induced by both endogenous

and exogenous catecholamines (12). Furthermore, considerable evidence exists that the effects of this catecholamine “surge” on the myocardium include an initial phase of regional depression of myocardial contractility (with minimal myocardial necrosis) followed by a prolonged phase of slowly resolving intense and essentially global myocardial inflammation and associated edema. Among systemic markers of myocardial inflammatory activation, substantial release of B-type natriuretic peptide/N-terminal pro-B-type natriuretic peptide in the absence of pulmonary edema serves best to delineate the progress of attacks (13). However, the precise cause of this inflammatory activation remains uncertain.

Studies in rodent models of TS have added substantially to the understanding of the impairment of myocardial contractility and associated propensity toward shock in the acute phases of the disorder. Notably, 2 studies have suggested a pivotal role for stimulation of  $\beta_2$ -adrenoceptors, with an associated shift from Gs- to Gi-based signal transduction, mediating cardiodepressant (but also cardioprotective) effects (14,15). However, the findings of these investigations do not address the issue of the pathogenesis of the myocardial inflammation that follows the initial catecholamine exposure, nor has any mechanism for inflammatory activation in TS been suggested by other previous experiments.

We made a series of observations which suggest that nitrosative stress may be critical to both inflammation and energetic impairment in TS. We showed

National Health and Medical Research Council (Australia). Mr. Surikow, Dr. Raman, and Dr. Singh were recipients of Postgraduate Research Scholarships from the University of Adelaide (Mr. Surikow and Dr. Singh) and from the Cardiac Society of Australia and New Zealand (Dr. Raman). The authors have reported that they have no relationships relevant to the contents of this paper to disclose. All authors attest they are in compliance with human studies committees and animal welfare regulations of the authors' institutions and Food and Drug Administration guidelines, including patient consent where appropriate. For more information, visit the *JACC: Basic to Translational Science* [author instructions page](#).

Manuscript received April 11, 2017; revised manuscript received October 8, 2017, accepted October 10, 2017.

that patients with TS differ from age-matched female control subjects with regard to 2 aspects of nitric oxide (NO) signaling (16). Specifically, patients with TS exhibited greater platelet responsiveness to the antiaggregatory effects of NO. Furthermore, plasma concentrations of asymmetric dimethylarginine, a competitive inhibitor of NO generation, were significantly lower in patients with TS than in control subjects. If release and/or effects of NO are increased in patients with TS, this result may be particularly relevant under conditions of  $\beta_2$ -adrenoceptor stimulation, given that  $\beta_2$ -adrenoceptors are coupled to activation of nitric oxide synthase (NOS) (17). Increased release of NO in the presence of the superoxide ( $O_2^-$ ) anion, which is also incrementally produced by the actions of catecholamines on the myocardium (18), potentially induces formation of the peroxynitrite ( $ONOO^-$ ) anion. This action induces associated redox stress, protein nitration (19), and deoxyribonucleic acid damage, resulting in activation of poly(ADP-ribose) polymerase (PARP)-1, which among other effects, acts as an “energy sink” (20); nicotinamide adenine dinucleotide is directly depleted, leading to potential phosphocreatine depletion, with associated inhibition of glycolysis (21).

Pilot immunohistological studies of LV myocardium in patients dying early in the course of TS indeed reported evidence of nitrosative stress: increased myocardial content of the nitrosative stress marker 3-nitrotyrosine (NT) and possibly increased content of poly(ADP-ribose) (PAR), a downstream product of PARP-1 activation (22), which represents a potential mechanism of energetic impairment (20,23).

We therefore sought to evaluate the potential roles of the generation of nitrosative stress, with the precursors of  $ONOO^-$  ( $O_2^-$  and NO) being incrementally generated by increased  $\beta_2$ -adrenoceptor stimulation (coupled to NOS activation [17]) and by oxidative stress induced primarily by catecholamine-triggered  $\beta_1$ -adrenoceptor stimulation and/or endothelial NOS “uncoupling,” respectively; a rat model of TS was utilized.

We also sought to evaluate the impact of this putative cascade on expression of the pro-inflammatory  $\alpha$ -arrestin thioredoxin-interacting protein (TXNIP), which might theoretically be increased either via direct stimulation by  $ONOO^-$  (24) and/or via withdrawal of NO-mediated suppression (25). Given that PARP-1 may activate nuclear factor kappa B (NF $\kappa$ B) (26) via phosphorylation, myocardial content of phosphorylated and total NF $\kappa$ B were also evaluated. The nature of the cellular component of myocardial inflammatory infiltrate in TS has been documented only minimally (8,27) thus far, and we also elected to evaluate those changes. Furthermore, in a subsequent

series of experiments, the impact of PARP-1 inhibition was evaluated to determine whether PARP-1 activation was mechanistically critical in this model.

## METHODS

**RAT MODEL.** The goal of this study was to assess the effects of isoproterenol on the myocardium of aging female rats ( $n = 17$ ; weight, 210 to 280 g) to most closely mimic the demographic characteristics of TS in humans. Preliminary experiments were conducted to assess the impact of age and dose of isoproterenol on tolerability; the results showed that in Sprague-Dawley rats age >8 months, the mortality rates after injection of isoproterenol were unacceptably high. Therefore, the age of 4 to 5 months and a dose of 5 mg/kg were eventually selected. Under these conditions, short-term mortality (manifest generally between 0.5 and 2 h) was approximately 33%. Baseline echocardiography was followed by a single intraperitoneal injection of isoproterenol for treated rats, with follow-up echocardiography performed 24 h later. Animals were then killed, and the myocardium was harvested for immunohistological and immunoblotting analyses. Control rats ( $n = 10$ ) were killed after 24 h, without exposure to isoproterenol, to provide immunohistochemical and immunoblotting controls. This study was approved by the relevant institutional ethics committees.

In a subsequent series of experiments, we evaluated the impact of pre-treatment with the PARP-1 inhibitor 3-aminobenzamide (3AB) (50 mg/kg intraperitoneal injection) administered 30 min before isoproterenol administration (ISO/3AB) ( $n = 17$ ). Comparisons were made with rats treated with isoproterenol alone (ISO) ( $n = 17$ ), blinded to treatment group. Four rats were treated with 3AB alone.

**Echocardiography.** For baseline and 24-h analysis of the effects of isoproterenol on LV structure and function, rats were initially anesthetized with 2% isoflurane, which was reduced to 0.5% during echocardiography. Animals were placed on their backs on a warming pad, their chest shaved and limb-leads attached for electrocardiogram recording. A Vivid 7 ultrasound system with a 10S 2298589 sector array probe (GE Vingmed Ultrasound AS, Horten, Norway), at a frequency of 4.0 to 10.5 MHz, was used for the acquisition of echocardiographic views. Views of the parasternal long-axis, as well as parasternal short-axis at the level of the base, mid, and apex, were captured for assessment of the left ventricle.

LV wall thickness and fractional area shortening were measured at end-diastole in the parasternal long-axis view, by using two-dimensional echocardiography, at 3 pre-defined levels: 1) basal, measurements were

performed at 3 mm below the mitral annulus; 2) mid-ventricle, measurements were recorded at the level of the papillary muscle; and 3) apical, measurements were performed 3 mm from the LV apex. Radial strain was measured from the short-axis view at the level of the apex with image depth set at approximately 2.0 to 2.5 cm with a frame rate of 240 to 260 frames/s.

Echocardiographic images were transferred to an EchoPAC PC workstation with Q analysis software enabled (GE Vingmed Ultrasound AS). Experienced investigators blinded to treatment status and phase of treatment performed all analyses, with measurements made in triplicate. Interobservation coefficient of variability for the measurement of apical strain was 13%.

**Preparation of rat myocardium.** After 24-h follow-up echocardiography, all rats were killed under anesthesia, and hearts were excised. Hearts were divided into basal and apical LV sections, which were fixed in 4% formaldehyde for paraffin embedding and snap-frozen in liquid nitrogen for immunoblotting analysis. **Immunohistological methods.** Myocardial content of the following was determined by immunohistochemistry: 1) 3-NT, as a marker of nitrosative stress; 2) PAR, representing the principal product of PARP-1 action; 3) TXNIP, a pro-inflammatory  $\alpha$ -arrestin; 4) CD68, as a marker of macrophage/monocyte infiltration; and 5) CD45, as a marker of leukocyte infiltration.

In all cases, the methods utilized for these studies were analogous, with variation only in the primary and secondary antibodies and dilution used. Thus, the sequence of quantitation involved the following steps. First, 4- $\mu$ m sections of tissue were cut and mounted onto Menzel Superfrost Ultra Plus (Thermo Fisher Scientific, Waltham, Massachusetts) slides, then allowed to dry overnight in a 37°C oven. Slides were deparaffinized, followed by antigen retrieval in citrate buffer at 100°C. Slides were blocked for endogenous peroxidase utilizing 3% hydrogen peroxide, followed by protein blocking using DAKO serum-free protein block (Agilent Technologies, Santa Clara, California). The primary antibodies were as follows: 3-NT (Upstate #06-284, Merck, Kenilworth, New Jersey), 1:500 dilution; PAR (Trevigen 4335-MC-100-AC, Bio-Techne, Minneapolis, Minnesota), 1:100 dilution; CD68 (ED1, Santa Cruz sc-59103, Dallas, Texas), 1:50 dilution and CD45 (OX30, Santa Cruz sc-53047), 1:25 dilution; and TXNIP (MBL Anti-TXNIP [VDUP1] mAb K0205-3, 1:500 dilution (Woburn, Massachusetts).

All primary antibodies were diluted in DAKO antibody diluent solution. Sections were left to incubate overnight at 4°C. The secondary antibody for 3-NT was DAKO EnVision+ System HRP Labelled Polymer

Anti-Rabbit (k4003), 1:100 dilution; for PAR, CD68, CD45, and TXNIP, Santa Cruz Biotechnology goat anti-mouse IgG-HRP (sc-2005), 1:100 dilution. Sections were left to incubate for 40 min at room temperature. For visualization, liquid DAB + Substrate Chromogen System (DAKO, k3467) was applied to each section, before being placed in distilled water to finish the reaction. Slides were incubated in hematoxylin for 10 s followed by 3 dips in Scott's Tap Water for counterstaining. Slides were then dehydrated, and coverslips were applied.

All slides are cleaned before being placed into the NanoZoomer (Hamamatsu Photonics K.K., Shizuoka Prefecture, Japan). Between 8 and 12 focus points were individually selected for each section, depending on the size of the section. NanoZoomer creates high-quality images of each section, allowing for accurate analysis.

All analyses were performed by investigators blinded as to rat treatment group. Reproducibility of estimates was evaluated via determination of the coefficient of variability. The images generated by NanoZoomer were processed by using Aperio ImageScope version 12.3 (Leica Biosystems, Nussloch, Germany), which generates a measure of the proportion of the total slide occupied by the stain.

**Immunoblotting studies.** Given the central importance of the 3-NT data, a subsidiary assay was performed by using immunoblotting (data on 5 control rats and 5 isoproterenol-treated rats, with blots in triplicate). Apical and basal sections of rat hearts were ground to a fine powder under liquid nitrogen and homogenized in 1X lysis buffer that contained protease and phosphatase inhibitor cocktails. The protein concentrations of supernatant were quantified in triplicate by using the DC Protein Assay (Bio-Rad Laboratories, Hercules, California) based on modification of the Lowry method and prepared in Laemmli sample buffer for separation at 30  $\mu$ g protein/sample. Proteins were separated by using a 7.6% sodium dodecyl sulfate polyacrylamide gel electrophoresis and transferred onto a nitrocellulose membrane (Sigma). Blots were blocked with 5% nonfat milk in Tris Buffered Saline, 0.01% Tween, at room temperature for 2 h and then probed overnight at 4°C using primary monoclonal antibodies (3-NT, Abcam, Cambridge, United Kingdom; ab61392, 1:4,000 dilution). The same blot was washed and re-probed for  $\beta$ -actin (Abcam, ab8226, 1:5,000 dilution for 3-NT) to determine equal sample to loading and then incubated with a secondary HRP-conjugated antibody (3-NT, Santa Cruz Biotechnology; anti-mouse 1:5,000 dilution). The bands were visualized by using ImageQuant LAS 4000 (GE Healthcare Life Sciences). Band intensities were

quantified by using Multi-Gauge Software. Effects on expression of 2 bands of 3-NT relative to  $\beta$ -actin were quantified for all experiments.

For subsequent experiments evaluating pre-treatment with 3AB, immunoblotting was also performed to compare expression of PARP-1 and its product PAR in hearts 24 h post-ISO (n = 10) or ISO/3AB (n = 10) treatment. The methods were as for 3-NT (detailed above) but utilizing the primary antibodies PARP (Cell Signaling Technologies, Danvers, Massachusetts; #9542: 1:1,000 dilution) and PAR (Trevigen; #4335-MC-100-AC: 1:800 dilution). The ratio of PAR generation to PARP-1 expression was used as a measure of PARP-1 activity.

Methods for NF $\kappa$ B were analogous to 3-NT and PARP/PAR, although with primary antibody for NF $\kappa$ B (Phosphorylated NF $\kappa$ B, Cell Signaling Technology; #3033 1:2,000; Total NF $\kappa$ B, Cell Signaling Technology, #8242 1:1,000). A dilution of 1:2,000 for  $\beta$ -actin was used, with secondary antibody at 1:5,000 (Santa Cruz Biotechnology, anti-rabbit). The ratio of phosphorylated NF $\kappa$ B to total NF $\kappa$ B was used as a measure of NF $\kappa$ B activation.

**STATISTICAL ANALYSIS.** All statistical analyses were performed by using GraphPad Prism 7.02 (GraphPad Software, La Jolla, California). Echocardiographic parameters were assessed via paired comparison of baseline and 24-h echocardiograms, with evaluation being performed while blinded as to experimental sequence. Comparisons of parameters were performed by using paired Student's *t* tests for normally distributed parameters.

Evaluation of differences in content and regional distribution (apical vs. basal myocardium) of 3-NT, TXNIP, and PAR was performed by using 2-way analysis of variance (ANOVA).

For evaluation in subsequent experiments of the impact of 3AB on ISO-induced changes, all statistical comparisons (unpaired) were between subsequently treated ISO rats and ISO/3AB-treated rats. Data involving effects of intervention (ISO or 3AB, respectively) on the difference between parameters at baseline and 24 h were normally distributed and were analyzed by using 2-way ANOVA. All data are expressed as mean  $\pm$  SEM unless otherwise stated.

## RESULTS

**EFFECTS OF ISO. Echocardiographic findings.** After injection of isoproterenol (5 mg/kg intraperitoneally), 11 of 28 rats died suddenly within 2 h; data for the surviving 17 rats were analyzed. Overall appearances of the left ventricle included a variable degree of apical hypokinesis. Major echocardiographic changes induced by isoproterenol are depicted in **Table 1**.

	Baseline	24 h	p Value
Heart rate, beats/min	336.4 $\pm$ 6.7	379.8 $\pm$ 8.1	0.0003
Apical wall thickness, mm	15.9 $\pm$ 0.4	19.5 $\pm$ 0.5	<0.0001
Apical strain rate, %	40.1 $\pm$ 1.6	24.7 $\pm$ 1.5	<0.0001
Apical fractional area shortening, %	50.0 $\pm$ 2.2	38.4 $\pm$ 2.5	0.0016
Ejection fraction, %	86.3 $\pm$ 1.0	82.0 $\pm$ 1.5	0.0075

Values are mean  $\pm$  SEM. Echocardiographic changes associated with intraperitoneal administration of isoproterenol (5 mg/kg, n = 17). The comparison is between pre-treatment status and 24 h post-isoproterenol.

Specifically, there was approximately a 15% increase in heart rate, apical LV wall thickness increased (consistent with the presence of myocardial edema), and apical strain rate decreased markedly (**Figure 1**), with a smaller, yet significant, decrease in apical fractional shortening and ejection fraction.

**Histology/immunohistochemistry.** The LV myocardium in isoproterenol-treated rats was infiltrated mainly with macrophages/monocytes (CD68+) rather than leukocytes (CD45+), consistent with activation of a cellular component of an inflammatory process (**Figure 2**).

3-NT accumulated significantly, especially in the apical myocardium (p = 0.0024) (**Figures 3A, 4A, and 4B**). There was approximately a 4-fold increase in 3-NT content (from 5.7  $\pm$  0.7% to 21.2  $\pm$  6.9%) of the apical myocardium of control rats compared with isoproterenol-treated animals.

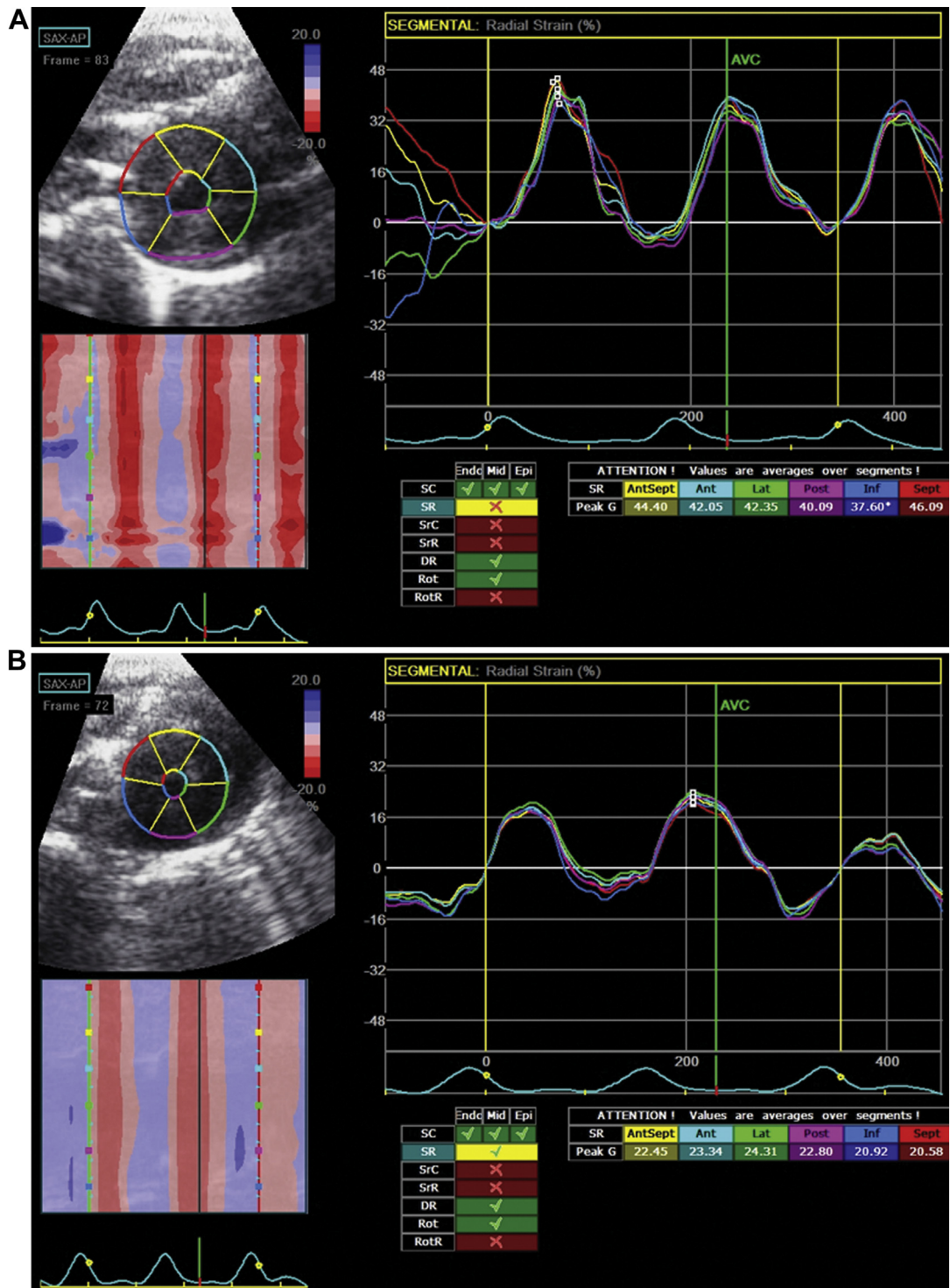
PAR content increased significantly (p = 0.014) (**Figures 3B, 4E, and 4F**), although less markedly than with 3-NT. For example, apical PAR content was 1.9  $\pm$  0.1% in control rats and 2.9  $\pm$  0.2% in isoproterenol-treated animals.

The TXNIP content of myocardium in isoproterenol-treated rats increased approximately 2.5-fold relative to control rats (**Figures 3C, 4C, and 4D**), with a significant apex-to-base gradient. Although this increase was not dissimilar to that seen with 3-NT, there was no significant correlation between 3-NT and TXNIP content.

**Immunoblotting.** 3-NT immunoblotting consistently generated 2 bands of molecular weight (47 and 70 kDa, respectively) (**Figure 5**), as shown in previous studies (28). Changes were quantitated regarding each individual band, rather than averaging data. These revealed (via 2-way ANOVA) a significant increase in the 47-kDa band (p = 0.003) and a borderline increase in the 70-kDa band (p = 0.05) with isoproterenol treatment without obvious regional variability.

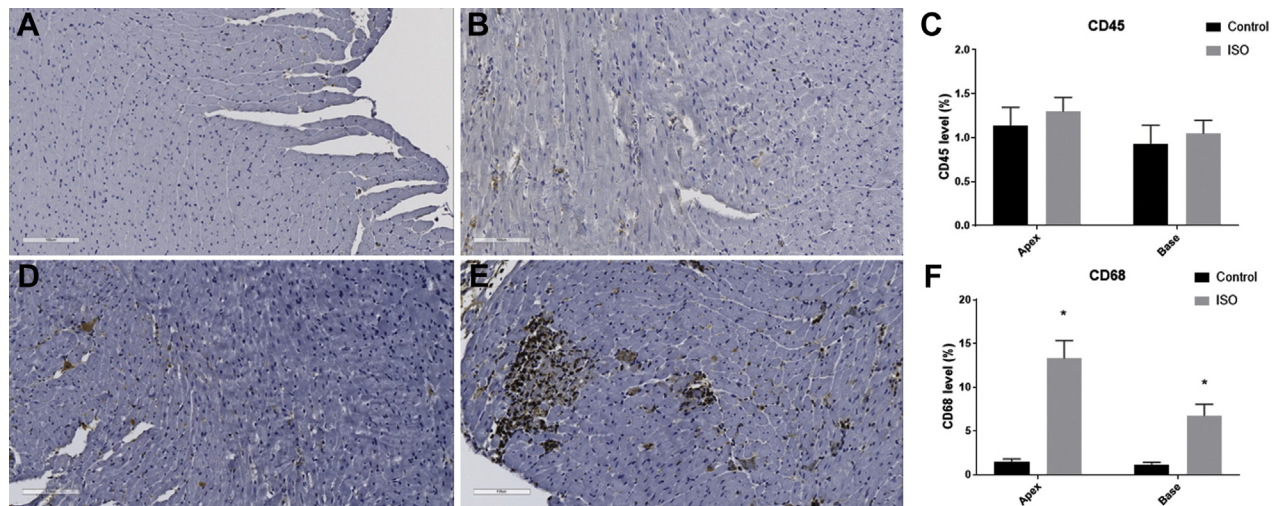
**COMPARISONS BETWEEN ISO AND ISO/3AB. Echocardiographic/clinical findings.** Mortality with ISO/3AB was approximately 32%, which is not significantly different from ISO alone. Data are presented on

**FIGURE 1** Functional Effects of ISO Alone



Echocardiographic strain data derived from apical myocardial motion in **(A)** pre-treated state and **(B)** 24-h post-injection of isoproterenol (ISO). Post-ISO analysis showed marked impairment of apical radial strain. Ant = anterior; AntSept = anteroseptal; AVC = aortic valve closure; Inf = inferior; Lat = lateral; Post = posterior; SAX-AP = short axis-apex; Sept = septal; SR = strain rate.

**FIGURE 2** Effects of ISO on Inflammatory Markers



Leukocyte infiltration, as measured by CD45, is shown in (A) control rat myocardium and (B) isoproterenol (ISO)-treated myocardium, with (C) summary data. Macrophage infiltration, measured with CD68 expression, is shown in (D) control rat myocardium and (E) ISO-treated myocardium, with (F) summary data. Five sections from each group were analyzed (20 sections in total); black/dark brown represents positive staining. \**p* < 0.05.

the 17 surviving rats. Apical radial strain and fractional shortening remained preserved in the ISO/3AB group at 24 h compared with the ISO alone group (time-treatment interaction values, *p* = 0.0004 and *p* = 0.037, respectively) (Table 2, Figure 6). Other echocardiographic measurements, such as apical wall thickness or heart rate, were not significantly different between the ISO alone and ISO/3AB groups.

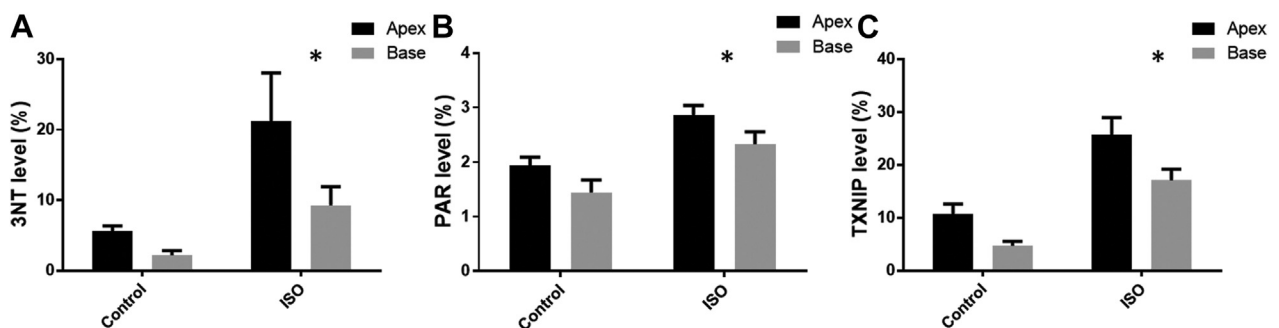
3AB alone induced no changes in wall motion (data not shown).

**Histology/immunohistochemistry.** CD68 content tended to decrease with ISO/3AB compared with ISO alone (mean 10.0 ± 3.3 to 7.2 ± 3.1), but this finding did not reach statistical significance.

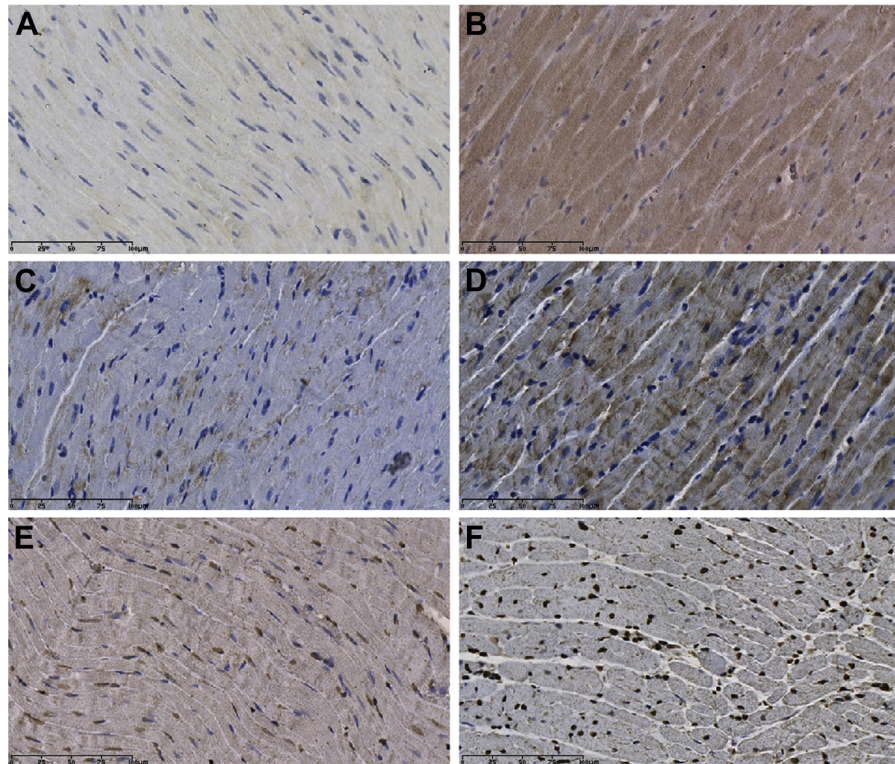
3-NT content was not significantly different between treatment groups at 24 h (treatment *p* > 0.05) (Figures 7A, 8A, and 8B).

PAR content was increased in the ISO/3AB group compared with the ISO alone group (treatment *p* = 0.0001) (Figures 7B, 8E, and 8F).

**FIGURE 3** Immunohistochemical Results for ISO Alone (Summative Data)



Effects of isoproterenol (ISO) on regional accumulation of 3-nitrotyrosine (3-NT), poly(ADP-ribose) (PAR), and thioredoxin-interacting protein (TXNIP) in left ventricular myocardium. (A) 3-NT mean values at apex and base. Two-way analysis of variance (ANOVA): ISO, *p* = 0.002; apex/base, *p* = 0.03; and interaction, *p* = 0.23. (B) PAR mean values at apex and base. Two-way ANOVA: ISO, *p* < 0.0001; apex/base, *p* = 0.01; and interaction, *p* = 0.93. (C) TXNIP mean values at apex and base. Two-way ANOVA: ISO, *p* < 0.0001; apex/base, *p* = 0.002; and interaction, *p* = 0.57. Two slides were analyzed per rat (apex and base); values are mean ± SEM. \**p* < 0.05.

**FIGURE 4 Immunohistochemical Effects of ISO Alone (Representative Images)**

Effects of ISO on 3-NT, TXNIP, and PAR expression in the myocardium. The accumulation of 3-NT is shown in (A) control rat myocardium and (B) ISO-treated myocardium. TXNIP accumulation is shown in (C) control rat myocardium and (D) ISO-treated myocardium. PAR accumulation is shown in (E) control rat myocardium and (F) ISO-treated myocardium. Abbreviations as in [Figure 3](#).

TXNIP content was further elevated in the myocardium of ISO/3AB-treated rats compared with rats receiving ISO alone (treatment  $p < 0.001$ ) ([Figures 7C, 8C, and 8D](#)).

**Immunoblotting.** PARP-1 immunoblotting (116-kD fragment) revealed that apical PARP-1 expression did not significantly differ at 24 h between ISO-treated rats and ISO/3AB-treated rats ( $6.9 \pm 2.7$  vs.  $2.1 \pm 0.8$ ; ANOVA,  $p = 0.16$ ).

PAR formation also did not change significantly ( $37.9 \pm 10.7$  for ISO and  $32.8 \pm 8$  for ISO/3AB;  $p = 0.90$ ).

Phosphorylated:total NF $\kappa$ B ratios were not significantly different between groups after performing a 2-way ANOVA with Dunnett's test for multiple comparisons ( $p = 0.43$ ).

## DISCUSSION

The current experiments were conducted to evaluate the possible occurrence, and potential

pathophysiological impact, of nitrosative stress in an animal model of TS. We showed, in female rats injected with isoproterenol, that precipitation of TS-like echocardiographic changes (29) was associated with intramyocardial accumulation of 3-NT, a conventional marker of nitrosative stress (19), and of PAR, a product of PARP-1 activation and thus a marker and mediator of myocardial energetic impairment (30). Myocardial TXNIP content was also significantly increased after ISO administration, consistent with increased stimuli for its expression, such as withdrawal of NO effect (25) and/or disruption of laminar flow and associated shear stress (31); this process known to be precipitated by glycocalyx shedding, a recently delineated component of TS (32). We also reported the presence of inflammatory infiltrate, with a substantial increase in CD68+ cells, representing predominantly macrophage/monocyte infiltration. Furthermore, as noted on echocardiography, LV wall thickness increased significantly with ISO. In a sequential series of experiments, the PARP-1 inhibitor 3AB substantially limited the severity of

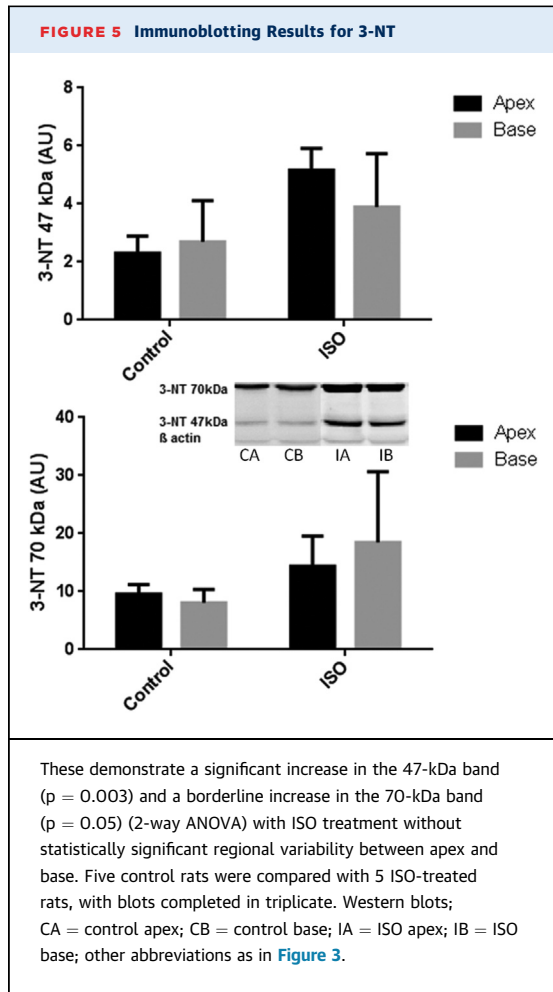


**TABLE 2 Echocardiographic Parameters for ISO Versus ISO/3AB**

	ISO		ISO/3AB		p Value
	Baseline	24 h	Baseline	24 h	
Heart rate, beats/min	336.4 ± 6.7	379.8 ± 8.1	347.5 ± 6.4	374.1 ± 5.4	0.21
Apical wall thickness, mm	15.9 ± 0.4	19.5 ± 0.5	15.4 ± 0.2	18.5 ± 0.4	0.64
Apical strain rate, %	40.1 ± 1.6	24.7 ± 1.5	42.7 ± 0.9	37.1 ± 1.1	0.0004
Apical fractional area shortening, %	50.0 ± 2.2	38.4 ± 2.5	46.4 ± 1.2	41.2 ± 1.2	0.001
Ejection fraction, %	86.3 ± 1.0	82.0 ± 1.5	83.6 ± 1.1	82.0 ± 1.1	0.25

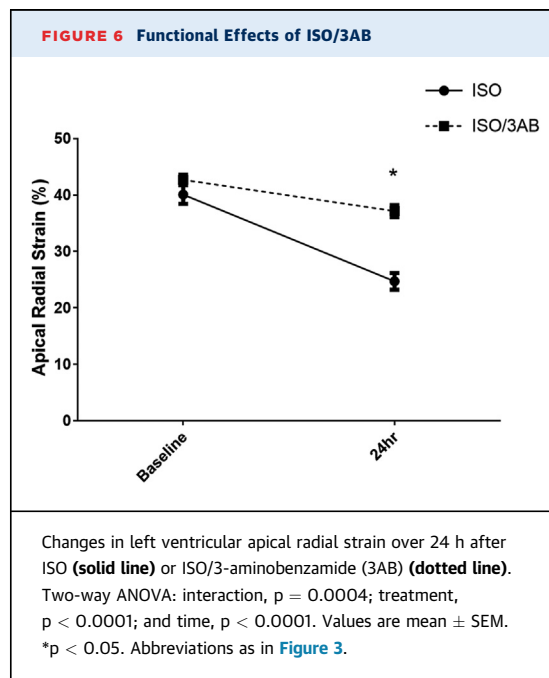
Values are mean ± SEM. Echocardiographic changes associated with intraperitoneal administration of isoproterenol alone (ISO: 5 mg/kg, n = 17) and isoproterenol + 3-aminobenzamide (ISO/3AB: 50 mg/kg, n = 17). Analysis is via 2-way analysis of variance, and p values are for time/treatment interaction.

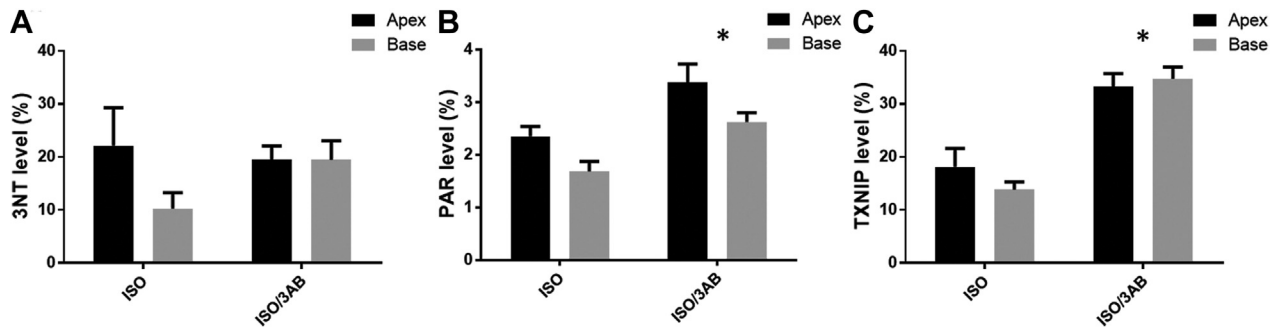
NOS (34);  $\beta_2$ -adrenoceptor stimulation would be expected to increase NO release in this manner. It has previously been shown that  $\beta_2$ -adrenoceptor density relative to that of  $\beta_1$ -adrenoceptors is greatest in the LV apical myocardium (15). In the rat ventricle,  $\beta$ -adrenoceptor-stimulated release of NO increases with senescence (35). Indeed, in the current experiments, even in control hearts, there was a trend for apical 3-NT content to exceed basal. In terms of the propensity for increased NO generation to induce nitrosative stress in the presence of oxidative stress, this factor has been previously shown in models of both central neuronal injury (36) and anthracycline-induced cardiac injury (37). Intriguingly, Zhang et al. (38) described the protective effects of hydrogen

systolic functional impairment in the rat model, relative to ISO alone.

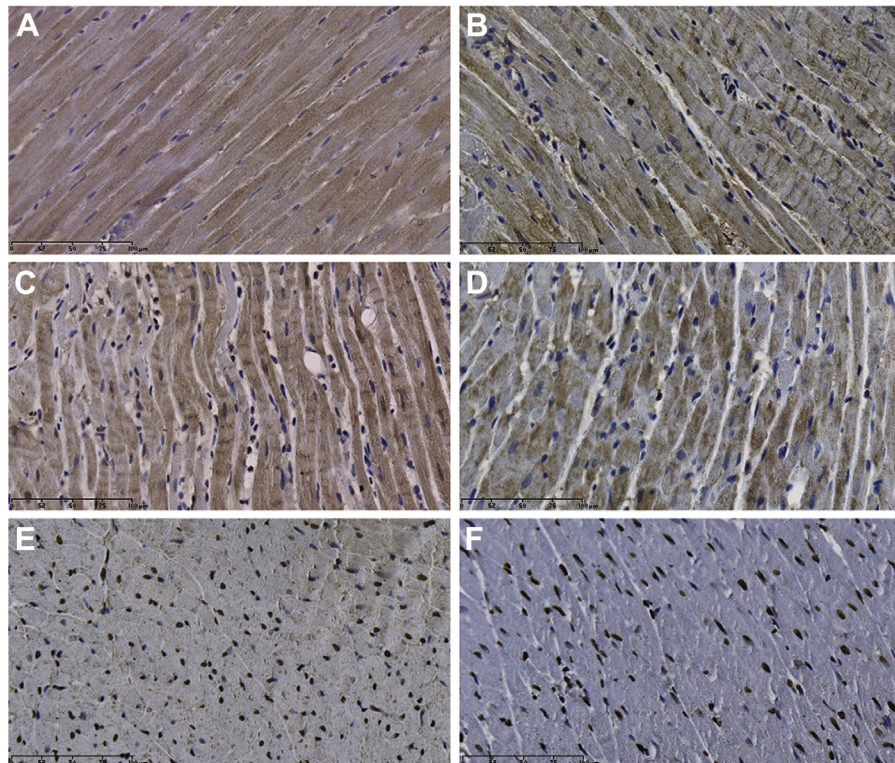
These findings are therefore consistent with four observations from our clinical investigations of TS. First, patients with TS usually have increased tissue responsiveness to NO and decreased concentrations of asymmetric dimethylarginine. These fluctuations facilitate ONOO<sup>-</sup> generation (19). Second, pilot studies in patients dying of TS also revealed increased myocardial 3-NT content (22). Third, myocardial energetic impairment persists for at least 4 months after acute attacks of TS (10). Finally, glycocalyx shedding occurs in the acute stages of TS (32), which increases cellular permeability and may contribute to the prolonged and characteristic accentuation of myocardial edema (33) in this condition. A schematic representation of these findings is provided in Figure 9.

The current findings are also consistent with the fact that myocardial  $\beta_2$ -adrenoceptors are linked to

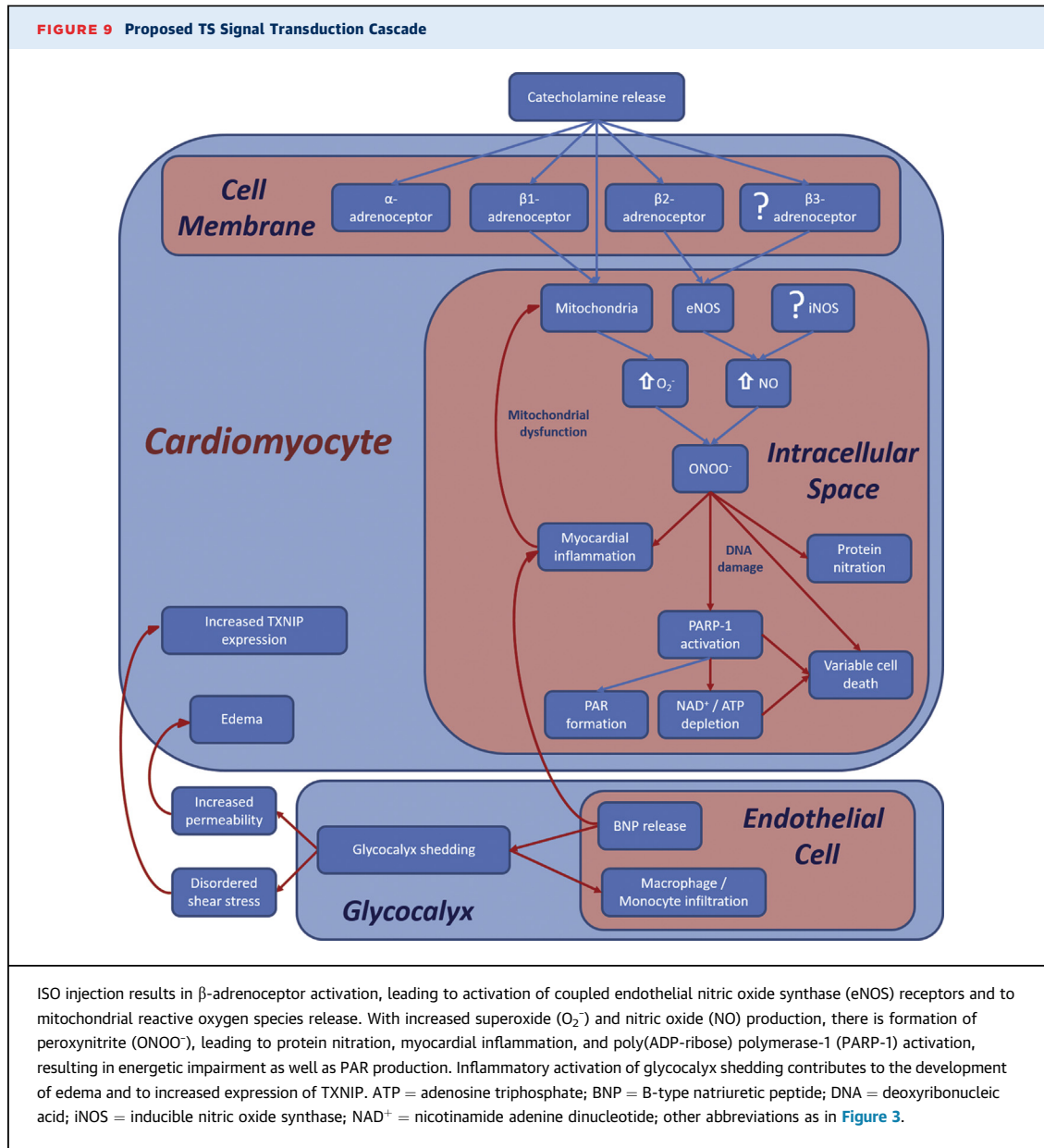


**FIGURE 7 Immunohistochemical Results for ISO Versus ISO/3AB (Summative Data)**

Effects of ISO on regional accumulation of 3-NT, PAR, and TXNIP in left ventricular myocardium with 3AB (ISO/3AB) and without (ISO). **(A)** 3-NT, showing mean values at apex and base. Two-way ANOVA: 3AB,  $p = 0.44$ ; apex/base,  $p = 0.17$ ; and interaction,  $p = 0.18$ . **(B)** PAR mean values at apex and base. Two-way ANOVA: 3AB,  $p = 0.0001$ ; apex/base,  $p = 0.0043$ ; and interaction,  $p = 0.86$ . **(C)** TXNIP mean values at apex and base. Two-way ANOVA: 3AB,  $p < 0.0001$ ; apex/base,  $p = 0.57$ ; and interaction,  $p = 0.26$ . Two slides were analyzed per rat (apex and base); values are mean  $\pm$  SEM. \* $p < 0.05$ . Abbreviations as in [Figures 3 and 6](#).

**FIGURE 8 Immunohistochemical Effects of ISO Versus ISO/3AB (Representative Images)**

Effects of ISO on 3-NT, TXNIP, and PAR expression in the myocardium, in the presence of ISO and in the absence of the poly(ADP-ribose) polymerase-1 inhibitor 3AB (ISO/3AB). 3-NT accumulation is shown in **(A)** ISO-treated myocardium and **(B)** ISO/3AB-treated myocardium. TXNIP accumulation is shown in **(C)** ISO-treated myocardium and **(D)** ISO/3AB-treated myocardium. PAR accumulation is shown in **(E)** ISO-treated myocardium and **(F)** ISO/3AB-treated myocardium. Abbreviations as in [Figures 3 and 6](#).



sulfide in isoproterenol-treated rats, a benefit apparently resulting from reversal of catecholamine-induced reactive oxygen species generation. However,  $ONOO^-$ -related markers were not assessed in this study.

The finding that the cellular myocardial infiltrate in this model consists primarily of macrophages/monocytes raises issues, including the basis for their presence within the myocardium and their potential contribution to myocardial cell damage. A previous study in an atherosclerotic mouse model

(39) found that macrophage/monocyte infiltration may result primarily from glycocalyx shedding, which itself is engendered largely by matrix metalloproteinase activation. Therefore, one potential means of evaluating this cascade of events ([Figure 9](#)) in terms of the impact on myocardial function would be to evaluate the effects of matrix metalloproteinase inhibitors (e.g., low-dose doxycycline) (40).

In view of the findings in the rats treated with isoproterenol alone, the question inevitably arises: is

nitrosative stress/PARP-1 activation pivotal to the development of the TS-like LV systolic dysfunction in this model?

We chose to address, in a subsequent series of rats, the hypothesis that the PARP-1 inhibitor 3AB might attenuate the contractile abnormalities seen with isoproterenol alone. In the event, 3AB did indeed significantly and markedly attenuate apical systolic dysfunction (Figure 6, Table 2). As expected from our overall construct (Figure 9), this finding was associated with no change in myocardial 3-NT content. In terms of the role of PARP-1 activity and formation of PAR, it must first be stated that in most models of acute cellular injury, PARP-1 activation is relatively transient, peaking within 4 h (41,42). Thus, the cardioprotective impact of 3AB would be exerted primarily during these first few hours. The observed increase in PAR content at 24 h (on immunohistochemical evaluation) suggests restoration of PAR formation after washout of 3AB. Indeed, Zhao et al. (43) have shown that in an acute myocardial infarction model, PARP protein expression level is increased for at least 8 weeks' post-administration of 3AB in association with acute infarction. From our immunoblotting data, it appears that there is little or no residual PARP-1 inhibition after 24 h. Furthermore, Cieslar-Pobuda et al. (41) have also documented evidence of precipitation of "rebound" oxidative stress 12 to 48 h post-pulse therapy with PARP-1 inhibitors. Taken together, these data suggest that reactivation of PARP-1 occurs under these circumstances, without limiting the overall utility of initial therapy.

The current results therefore represent the most definitive evidence to date of a central role for nitrosative stress in a model of TS. However, it remains to be determined in the clinical setting to what extent PARP-1 activation post- $\beta_2$ -adrenoceptor stimulation contributes to the prolonged energetic impairment that has recently been demonstrated clinically in TS (10). For example, it is theoretically possible that increased TXNIP content may have contributed to energetic impairment as well as to overall inflammatory activation (31).

Activation of PARP-1, apart from its role in deoxyribonucleic acid repair, also functions as an "energetic sink," depleting adenosine triphosphate (20) and inhibiting glycolysis (21) during the production of PAR. If this effect is central to the impairment of myocardial contractility, it would be expected that inhibition of either the ONOO<sup>-</sup> effect (44) or of PARP-1 (23) would ameliorate TS. Both

experimentally and clinically based investigations to evaluate this possibility seem appropriate under the current circumstances. In this regard, the finding on meta-analysis that utilization of angiotensin-converting enzyme inhibitors (which limit PARP-1 activation [45]) may limit recurrence of TS (46) is consistent with a known effect on nitrosative stress (47).

**STUDY LIMITATIONS.** There are several limitations to the current study, beginning with those inherent in an animal model. We investigated only single doses of isoproterenol and 3AB, with a single post-intervention time point (while both earlier and later evaluation might well have been useful), and therefore needed only a relatively small sample size. Furthermore, although we detected nitrosative stress, we have not yet determined whether the observed negative inotropic changes might also partially reflect ONOO<sup>-</sup>-mediated effects, independent of PARP-1 activation (44). We have also not determined to what extent the observed contractile changes in this model are initiated by  $\beta$ -adrenoceptor-triggered NOS activation.

It is important to recognize that 3AB limited, but did not totally abolish, the negative inotropic effects of isoproterenol. Hence, it is possible that other biochemical mediators may contribute to these changes. For example, Willis et al. (48) used a rat model similar to that in the current study but evaluated residual impairment of contractility after 2 weeks. At that stage, both impaired oxidative metabolism and calcium mishandling in both systole and diastole were shown to underlie contractile impairment.

The extent of myocardial edema associated with the acute increase in LV wall thickness was not determined, and therefore it is uncertain to what extent this finding might have been due to swelling of inflamed myocardial cells. Other studies have reported, for example, increased cardiomyocyte diameter (49) and/or increased cardiac weight (50) without specifically investigating the potential role of increased tissue fluid load; further clarification of this issue is therefore a priority. In terms of the potential duration of inflammatory changes post-isoproterenol administration, a number of studies (50,51) have evaluated the impact of prolonged isoproterenol administration in the rat model, documenting a plateau effect early regarding negative inotropy and a diminution of presumptive inflammation/edema after day 1.

## CONCLUSIONS

Until recently, it might have been considered that TS was relatively rare and generally benign; the lack of an effective treatment was therefore of little importance. With greater understanding of the natural history of this disorder (33,52), and of the role of nitrosative stress in the pathogenesis of TS (Figure 9), it has become necessary to develop appropriate strategies to treat the myocardial inflammatory activation that drives the clinical features of TS.

**ACKNOWLEDGMENTS** The authors thank Cher-Rin Chong and Geraldine Murphy for their invaluable assistance with the immunohistochemical analyses, along with Matthew Smith for his assistance with animal handling. They also thank Professor Danny Liew of the Outcome Research Unit, Monash University, for his invaluable contribution to the statistical analyses.

**ADDRESS FOR CORRESPONDENCE:** Dr. John D. Horowitz, Cardiology Unit, The Queen Elizabeth Hospital, 28 Woodville Road, Woodville South, SA 5011, Australia. E-mail: [john.horowitz@adelaide.edu.au](mailto:john.horowitz@adelaide.edu.au).

## PERSPECTIVES

**COMPETENCY IN MEDICAL KNOWLEDGE:** Although it is now clear that TS is a relatively common cause of disability and death, especially in aging women, there is no current consensus as to how, in susceptible hearts, catecholamine exposure induces inflammatory activation within the myocardium, with systolic dysfunction and associated energetic impairment. Despite its substantial long-term mortality rate, TS has no established treatment. However, the presence of nitrosative stress, previously reported in post-mortem heart samples, represents a theoretical basis for therapeutic intervention.

**TRANSLATIONAL OUTLOOK:** We found that in hearts of female rats, exposure to  $\beta_2$ -adrenoceptor stimulation induces TS-like ventricular dysfunction, nitrosative stress, and downstream activation of the "energetic sink" enzyme PARP-1. These findings raise a number of potential therapeutic options for both acute management and long-term treatment post-TS, including inhibition of NOS, "scavenging" of ONOO<sup>-</sup>, PARP-1 inhibition, and use of angiotensin-converting enzyme inhibitors.

## REFERENCES

1. Sato H, Tateishi H, Uchida T. Tako-tsubo-like Left Ventricular Dysfunction due to Multivessel Coronary Spasm. Clinical Aspect of Myocardial Injury: From Ischemia to Heart Failure. Tokyo, Japan: Kagakuhyoronsha Publishing Co, 1990: 56-64. In Japanese.
2. Sharkey SW, Windenburg DC, Lesser JR, et al. Natural history and expansive clinical profile of stress (Tako-Tsubo) cardiomyopathy. *J Am Coll Cardiol* 2010;55:333-41.
3. Lyon AR, Bossone E, Schneider B, et al. Current state of knowledge on Takotsubo syndrome: a position statement from the Taskforce on Takotsubo Syndrome of the Heart Failure Association of the European Society of Cardiology. *Eur J Heart Fail* 2016;18:8-27.
4. Templin C, Ghadri JR, Diekmann J, et al. Clinical features and outcomes of Takotsubo (stress) cardiomyopathy. *N Engl J Med* 2015;373: 929-38.
5. Jaguszewski M, Osipova J, Ghadri JR, et al. A signature of circulating microRNAs differentiates Takotsubo cardiomyopathy from acute myocardial infarction. *Eur Heart J* 2014;35:999-1006.
6. Raman B, Singh K, Zeitz CJ, Horowitz JD. Takotsubo cardiomyopathy presenting as S-T elevation myocardial infarction: not gone but forgotten? *Int J Cardiol* 2014;172:e261-2.
7. Neil C, Nguyen TH, Kucia A, et al. Slowly resolving global myocardial inflammation/oedema in Tako-Tsubo cardiomyopathy: evidence from T2-weighted cardiac MRI. *Heart* 2012;98: 1278-84.
8. Wittstein IS, Thiemann DR, Lima JA, et al. Neurohumoral features of myocardial stunning due to sudden emotional stress. *N Engl J Med* 2005;352:539-48.
9. Neil CJ, Nguyen TH, Singh K, et al. Relation of delayed recovery of myocardial function after Takotsubo cardiomyopathy to subsequent quality of life. *Am J Cardiol* 2015;115:1085-9.
10. Dawson DK, Neil CJ, Henning A, et al. Tako-Tsubo cardiomyopathy: a heart stressed out of energy? *J Am Coll Cardiol Img* 2015;8:985-7.
11. Singh K, Carson K, Usmani Z, Sawhney G, Shah R, Horowitz J. Systematic review and meta-analysis of incidence and correlates of recurrence of Takotsubo cardiomyopathy. *Int J Cardiol* 2014; 174:696-701.
12. Lyon AR, Rees PS, Prasad S, Poole-Wilson PA, Harding SE. Stress (Takotsubo) cardiomyopathy—a novel pathophysiological hypothesis to explain catecholamine-induced acute myocardial stunning. *Nat Clin Pract Cardiovasc Med* 2008;5:22-9.
13. Nguyen TH, Neil CJ, Sverdlow AL, et al. N-terminal pro-brain natriuretic protein levels in Takotsubo cardiomyopathy. *Am J Cardiol* 2011; 108:1316-21.
14. Shao Y, Redfors B, Scharin Tang M, et al. Novel rat model reveals important roles of beta-adrenoreceptors in stress-induced cardiomyopathy. *Int J Cardiol* 2013;168:1943-50.
15. Paur H, Wright PT, Sikkil MB, et al. High levels of circulating epinephrine trigger apical cardiodepression in a beta2-adrenergic receptor/Gi-dependent manner: a new model of Takotsubo cardiomyopathy. *Circulation* 2012;126: 697-706.
16. Nguyen TH, Neil CJ, Sverdlow AL, et al. Enhanced NO signaling in patients with Takotsubo cardiomyopathy: short-term pain, long-term gain? *Cardiovasc Drugs Ther* 2013;27:541-7.
17. Ferro A, Coash M, Yamamoto T, Rob J, Ji Y, Queen L. Nitric oxide-dependent beta2-adrenergic dilatation of rat aorta is mediated through activation of both protein kinase A and Akt. *Br J Pharmacol* 2004;143:397-403.
18. Liang Y, Liu D, Ochs T, et al. Endogenous sulfur dioxide protects against isoproterenol-induced myocardial injury and increases myocardial antioxidant capacity in rats. *Lab Invest* 2011; 91:12-23.
19. Mukhopadhyay P, Rajesh M, Batkai S, et al. Role of superoxide, nitric oxide, and peroxynitrite in doxorubicin-induced cell death in vivo and in vitro. *Am J Physiol Heart Circ Physiol* 2009;296: H1466-83.
20. Luo X, Kraus WL. On PAR with PARP: cellular stress signaling through poly(ADP-ribose) and PARP-1. *Genes Dev* 2012;26:417-32.
21. Andrabi SA, Umanah GK, Chang C, et al. Poly(ADP-ribose) polymerase-dependent energy depletion occurs through inhibition of glycolysis. *Proc Natl Acad Sci U S A* 2014;111:10209-14.
22. Surikow SY, Raman B, Licari J, Singh K, Nguyen TH, Horowitz JD. Evidence of nitrosative stress within hearts of patients dying of Takotsubo cardiomyopathy. *Int J Cardiol* 2015;189: 112-4.

23. Virag L, Szabo C. The therapeutic potential of poly(ADP-ribose) polymerase inhibitors. *Pharmacol Rev* 2002;54:375-429.
24. Forrester MT, Seth D, Hausladen A, et al. Thioredoxin-interacting protein (Txnip) is a feedback regulator of S-nitrosylation. *J Biol Chem* 2009;284:36160-6.
25. Schulze PC, Liu H, Choe E, et al. Nitric oxide-dependent suppression of thioredoxin-interacting protein expression enhances thioredoxin activity. *Arterioscler Thromb Vasc Biol* 2006;26:2666-72.
26. Hassa PO, Hottiger MO. The functional role of poly(ADP-ribose)polymerase 1 as novel coactivator of NF-kappaB in inflammatory disorders. *Cell Mol Life Sci* 2002;59:1534-53.
27. Nef HM, Mollmann H, Kostin S, et al. Takotsubo cardiomyopathy: intraindividual structural analysis in the acute phase and after functional recovery. *Eur Heart J* 2007;28:2456-64.
28. Rogers NM, Thomson AW, Isenberg JS. Activation of parenchymal CD47 promotes renal ischemia-reperfusion injury. *J Am Soc Nephrol* 2012;23:1538-50.
29. Redfors B, Ali A, Shao Y, Lundgren J, Gan LM, Omerovic E. Different catecholamines induce different patterns of Takotsubo-like cardiac dysfunction in an apparently afterload dependent manner. *Int J Cardiol* 2014;174:330-6.
30. Ying W, Chen Y, Alano CC, Swanson RA. Tricarboxylic acid cycle substrates prevent PARP-mediated death of neurons and astrocytes. *J Cereb Blood Flow Metab* 2002;22:774-9.
31. Chong CR, Chan WP, Nguyen TH, et al. Thioredoxin-interacting protein: pathophysiology and emerging pharmacotherapeutics in cardiovascular disease and diabetes. *Cardiovasc Drugs Ther* 2014; 28:347-60.
32. Nguyen TH, Liu S, Ong GJ, Stafford I, Frenneaux MP, Horowitz JD. Glycocalyx shedding is markedly increased during the acute phase of Takotsubo cardiomyopathy. *Int J Cardiol* 2017;243:296-9.
33. Akashi YJ, Nef HM, Lyon AR. Epidemiology and pathophysiology of Takotsubo syndrome. *Nat Rev Cardiol* 2015;12:387-97.
34. Zhu WZ, Zheng M, Koch WJ, Lefkowitz RJ, Kobilka BK, Xiao RP. Dual modulation of cell survival and cell death by beta(2)-adrenergic signaling in adult mouse cardiac myocytes. *Proc Natl Acad Sci U S A* 2001;98:1607-12.
35. Birenbaum A, Tesse A, Loyer X, et al. Involvement of beta 3-adrenoceptor in altered beta-adrenergic response in senescent heart: role of nitric oxide synthase 1-derived nitric oxide. *Anesthesiology* 2008;109:1045-53.
36. Hortobagyi T, Gorchach C, Benyo Z, et al. Inhibition of neuronal nitric oxide synthase-mediated activation of poly(ADP-ribose) polymerase in traumatic brain injury: neuroprotection by 3-aminobenzamide. *Neuroscience* 2003;121:983-90.
37. Fogli S, Nieri P, Breschi MC. The role of nitric oxide in anthracycline toxicity and prospects for pharmacologic prevention of cardiac damage. *FASEB J* 2004;18:664-75.
38. Zhang Z, Jin S, Teng X, Duan X, Chen Y, Wu Y. Hydrogen sulfide attenuates cardiac injury in Takotsubo cardiomyopathy by alleviating oxidative stress. *Nitric Oxide* 2017;67:10-25.
39. Cancel LM, Ebong EE, Mensah S, Hirschberg C, Tarbell JM. Endothelial glycocalyx, apoptosis and inflammation in an atherosclerotic mouse model. *Atherosclerosis* 2016;252:136-46.
40. Lipowsky HH, Lescanic A. The effect of doxycycline on shedding of the glycocalyx due to reactive oxygen species. *Microvasc Res* 2013;90: 80-5.
41. Cieslar-Pobuda A, Saenko Y, Rzeszowska-Wolny J. PARP-1 inhibition induces a late increase in the level of reactive oxygen species in cells after ionizing radiation. *Mutat Res* 2012;732:9-15.
42. Uchida K, Takahashi S, Fujiwara K, et al. Preventive effect of 3-aminobenzamide on the reduction of NAD levels in rat liver following administration of diethylnitrosamine. *Jpn J Cancer Res* 1988;79:1094-100.
43. Zhao YJ, Wang JH, Fu B, et al. Effects of 3-aminobenzamide on expressions of poly(ADP-ribose) polymerase and apoptosis inducing factor in cardiomyocytes of rats with acute myocardial infarction. *Chin Med J (Engl)* 2009;122:1322-7.
44. Szabo G, Loganathan S, Merkely B, et al. Catalytic peroxynitrite decomposition improves reperfusion injury after heart transplantation. *J Thorac Cardiovasc Surg* 2012;143:1443-9.
45. Pacher P, Szabo C. Role of poly(ADP-ribose) polymerase-1 activation in the pathogenesis of diabetic complications: endothelial dysfunction, as a common underlying theme. *Antioxid Redox Signal* 2005; 7:1568-80.
46. Singh K, Carson K, Shah R, et al. Meta-analysis of clinical correlates of acute mortality in Takotsubo cardiomyopathy. *Am J Cardiol* 2014;113: 1420-8.
47. Pacher P, Obrosova IG, Mabley JG, Szabo C. Role of nitrosative stress and peroxynitrite in the pathogenesis of diabetic complications. Emerging new therapeutical strategies. *Curr Med Chem* 2005;12:267-75.
48. Willis BC, Salazar-Cantu A, Silva-Platas C, et al. Impaired oxidative metabolism and calcium mishandling underlie cardiac dysfunction in a rat model of post-acute isoproterenol-induced cardiomyopathy. *Am J Physiol Heart Circ Physiol* 2015;308:H467-77.
49. Mueller KAL, Heinzmann D, Klingel K, et al. Histopathological and immunological characteristics of tachycardia-induced cardiomyopathy. *J Am Coll Cardiol* 2017;69:2160-72.
50. Krenek P, Kmecova J, Kucerova D, et al. Isoproterenol-induced heart failure in the rat is associated with nitric oxide-dependent functional alterations of cardiac function. *Eur J Heart Fail* 2009;11:140-6.
51. Linck B, Boknik P, Baba HA, et al. Long-term beta adrenoceptor-mediated alteration in contractility and expression of phospholamban and sarcoplasmic reticulum Ca(++)-ATPase in mammalian ventricle. *J Pharmacol Exp Ther* 1998; 286:531-8.
52. Yoshikawa T. Takotsubo cardiomyopathy, a new concept of cardiomyopathy: clinical features and pathophysiology. *Int J Cardiol* 2015;182: 297-303.

---

**KEY WORDS** myocardial inflammation, oxidative stress, poly(ADP-ribose) polymerase-1, Takotsubo cardiomyopathy